



HAL
open science

Solid dispersions of quercetin-PEG matrices: Miscibility prediction, preparation and characterization

Elisabeth van Hecke, Mohammed Benali

► To cite this version:

Elisabeth van Hecke, Mohammed Benali. Solid dispersions of quercetin-PEG matrices: Miscibility prediction, preparation and characterization. Food Bioscience, 2022, 49, pp.101868. 10.1016/j.fbio.2022.101868 . hal-04709487

HAL Id: hal-04709487

<https://hal.science/hal-04709487v1>

Submitted on 13 Nov 2024

HAL is a multi-disciplinary open access archive for the deposit and dissemination of scientific research documents, whether they are published or not. The documents may come from teaching and research institutions in France or abroad, or from public or private research centers.

L'archive ouverte pluridisciplinaire **HAL**, est destinée au dépôt et à la diffusion de documents scientifiques de niveau recherche, publiés ou non, émanant des établissements d'enseignement et de recherche français ou étrangers, des laboratoires publics ou privés.



Distributed under a Creative Commons Attribution - NonCommercial 4.0 International License

11 **Solid dispersions of quercetin-PEG matrices: Miscibility prediction,**
12 **preparation and characterization**

13
14
15
16 **ABSTRACT**

17 Quercetin is a bioflavonoid compound with low water solubility in both foods and the gastrointestinal
18 tract, which limits the exploitation of its health-promoting properties. This study aims to formulate solid
19 dispersions (SDs) of quercetin with hydrophilic polyethylene glycol PEG matrices, using the melt-
20 mixing method, to improve the dissolution and antioxidant activity of quercetin. Initially, the total Gibbs
21 free energy for different binary mixtures was modelled to predict the miscibility of the compounds.
22 Then, the physicochemical properties of the formulated SDs were characterised and dissolution tests and
23 antioxidant activity measurements were performed in vitro to evaluate the improved profiles and
24 antioxidant activity of the SDs developed. The group contribution methods of Hoy and Van Krevelen
25 and Hoftyzer, used for PEG solubility parameter calculations, presented a suitable prediction of
26 interaction and miscibility behaviour. The results suggested the presence of amorphous quercetin
27 precipitates in the crystalline matrix of PEG 4000 and PEG 6000, and the formation of an amorphous
28 SD between quercetin and PEG 1000. These formulations achieved good radical scavenging activity and
29 better dissolution, especially the quercetin-PEG 1000 SDs.

30
31 **Keywords:** solid dispersion; quercetin; PEG; solubility parameters; miscibility; radical scavenging
32 activity

33 **1 Introduction**

34 Flavonoids are natural substances with a wide range of uses, including biotechnology, nutraceuticals,
35 and the development of novel bioactive compounds, co-drugs, chemo-protectors, and herbal medicines.
36 Flavonoids are divided into several classes that differ in the degree of saturation of the aglycone
37 heterocycle, its oxidation, and spatial conformation. Among these classes, we find flavanols,
38 anthocyanidins, and flavonols.

39 Quercetin, *2-(3,4-dihydroxyphenyl)-3,5,7-trihydroxychromen-4-one*, is classified as a flavonol and is a
40 major compound of polyphenolic bioflavonoid (El-Saber Batiha et al., 2020). It has been reported that
41 quercetin has several potentially beneficial health effects, including antioxidant, anti-carcinogenic, and
42 anti-hypertensive activities. Recently, quercetin has been reported as exhibiting synergistic antiviral
43 effects when ingested with vitamin C, which may help relieve some of the symptoms associated with
44 COVID-19 (Chow et al., 2020).

45 In fruits, vegetables or plant extracts, quercetin is found as glycosides with a sugar fraction attached to
46 one of the hydroxyl groups, increasing their solubility in water, such as quercetin glycosides,
47 isoquercetin, and rutin. Thus, quercetin is ingested in the form of glycosides and is then found in the
48 aglycone form in the gastrointestinal tract after hydrolysis. However, quercetin-aglycones have lower
49 bioavailability and solubility in water and the human gut (El-Saber Batiha et al., 2020).

50 To improve the solubility and bioavailability of quercetin while preserving its activity, various methods
51 and efforts have been deployed, such as encapsulation in nanoparticles (Zou et al., 2021), particle size
52 reduction (Manca et al., 2020), emulsification (Khalid et al., 2016), complexation with cyclodextrins
53 (Yang et al., 2019), and solid dispersions (Gilley et al., 2017). The solid dispersion (SD) method is
54 usually used to enhance low solubility bioactive compounds' release rate and bioavailability. The solid
55 dispersion formulation combines two distinct components: the hydrophobic bioactive compound and the
56 hydrophilic carrier matrix. Solid dispersions were classified according to the state of both bioactive
57 compound and carrier matrix: eutectic mixtures, crystalline or amorphous solid dispersions, and solid
58 solutions (Shah et al., 2014). In the pharmaceutical sector, the first generation of solid dispersions used
59 crystalline carriers and three types of solid dispersions were obtained differently in the bioactive
60 compound or the drug: crystalline compound (eutectic solid dispersion), amorphous compound
61 (amorphous precipitates in the crystalline matrix), or molecularly dissolved (solid solutions) state. The
62 second-generation used natural or synthetic amorphous polymer supports, with drugs in crystalline
63 (glass suspension), amorphous (amorphous solid dispersion), or molecularly dissolved (glass solution)
64 form.

65 Generally, the solid dispersion of a poorly water-soluble molecule in a hydrophilic carrier (amorphous
66 or crystalline) increases the dissolution behaviour of the hydrophobic compound when this system is
67 exposed to water. This is attributed to several factors, such as improved wettability of the drug by the
68 polymer, reduced particle size, separation of individual drug particles by polymer particles, changing the
69 drug from a crystalline to an amorphous state, and the subsequent prevention of precipitation of the drug
70 in contact with aqueous media (Shah et al., 2014). There are various techniques for preparing the solid
71 dispersion of hydrophobic compounds to improve their aqueous solubility: the solvent evaporation
72 method, hot-melt extrusion, and the melting method (Shah et al., 2014). The main advantages of the
73 latter method of fusion are that it is solvent-free. An important condition for the formation of solid

74 dispersion using the fusion method is the miscibility of the hydrophobic compound and matrix in molten
75 form. Another important condition is the thermostability of the bioactive compounds and hydrophilic
76 matrix.

77 To obtain a solid dispersion containing the solute or hydrophobic bioactive compound in a stable
78 amorphous state, the two components must be thermodynamically miscible during the process; ideally,
79 this miscibility must be maintained under storage conditions. In the case of liquid mixtures, the balance
80 between the entropy and enthalpy of the mixture, and therefore the free energy of mixing, dictates
81 miscibility. Based on the concepts of statistical thermodynamics, Flory and Huggins (Ulrich, 1978)
82 proposed modifications to the original regular solution theory to make it applicable to a polymer-solvent
83 binary system. The Flory-Huggins theory of polymer solutions provides an expression for calculating
84 the overall free energy of dissolution per mole of lattice site and is very effective for predicting the
85 behaviour of polymer-solvent systems. This theory was later extended to the drug-polymer system and
86 has demonstrated its usefulness in describing their miscibility by taking into account the large size
87 difference between the two components (Baird & Taylor, 2012; Shah et al., 2014).

88 The Flory-Huggins equation for calculating the total Gibbs free energy of mixing, $\Delta G_m(J)$, of a drug-
89 polymer system, leads to the following expression:

$$90 \quad \frac{\Delta G_m}{RT} = [n_d \ln \phi_d + n_p \ln \phi_p] + [n_d \phi_p \chi_{dp}] \quad (1)$$

91

92 where R is gas constant ($J.mol^{-1}.K^{-1}$), T absolute temperature (K), n_s and ϕ_s number of moles and
93 volume fraction

94 solute, whereas n_p and ϕ_p are the number of moles and volume fraction of polymer respectively; χ_{dp} is
95 the Flory-Huggins interaction parameter, which represents the interaction between polymer segments
96 and solute molecules.

97 In this expression, the first term on the right-hand side of the equation represents the entropy of mixing,
98 (ΔS_m) and the second term represents the enthalpy of mixing (ΔH_m). A necessary condition for
99 miscibility is that the total Gibbs free energy of mixing should be less than 0. When mixing solutes,
100 especially bioactive molecules or drugs, with a polymer, the entropy contribution will always favour
101 mixing, depending on polymer molecular weight with respect to the drug molar weight. In contrast, it is
102 the enthalpic component of the free energy of mixing that will determine whether $\Delta G_m \leq 0$ or not, and
103 hence whether mixing is going to occur or not (Marsac et al., 2006). Therefore, to predict miscibility
104 between a solute and a polymer, it is necessary to estimate the magnitude of the interaction parameter
105 χ_{dp} . One of the different approaches used for estimating the polymer χ_{dp} is the one based on the
106 solubility parameter of solute δ_s and of polymer matrix δ_m as shown in the following equation:

$$107 \quad \chi_{dp} = V \frac{(\delta_s - \delta_m)^2}{RT} \quad (2)$$

108

109 where V is the volume of the hypothetical lattice.

110 The equation above shows that two substances exhibiting a similar numerical value of solubility
111 parameter are expected to undergo mutual mixing, whereas a higher difference between the values of δ_s
112 and δ_m indicates decreased tendency to undergo mixing. It has been noted that Eq. (2) would generally
113 be sufficient for systems with van der Waals interactions, but not for systems with specific directional

114 interactions such as hydrogen bonding (Marsac et al., 2006).
115 In the present study, polyethylene glycol, with molecular weights from 1000 to 6000 was used, because
116 it has high solubility in water, good stability and a relatively low melting point, around 35-70°C.
117 Polyethylene glycol (PEG) is one of the matrices commonly used in solid dispersion. It has been
118 reported that solid dispersion using PEGs increases the solubility of poorly soluble flavonoids such as
119 naringin, hesperidin, hesperetin (Kanaze et al., 2006) and luteolin (Alshehri et al., 2020).
120 To our knowledge, no study has been carried out regarding the effect of PEG molecular weights (Mw)
121 between 1000 and 6000 on the enhancement of quercetin dissolution in solid dispersion, using the melt
122 mixing method in a high-speed disperser process. This study aims to investigate the effect of PEG
123 molecular weights on the miscibility and structures of quercetin precipitate, crystalline or amorphous, in
124 solid dispersion. To extract information about the effect of PEG molecular weights on the interaction
125 and compatibility in quercetin-PEG solid dispersions, the total Gibbs free energy of mixing for different
126 binary mixtures was modelled using the solubility parameter. Then, the physicochemical and stability
127 properties of the solid dispersions formulated were characterized and compared using instrumental
128 analysis: Fourier transform infrared (FTIR) spectroscopy, powder X-ray diffraction (XRD), differential
129 scanning calorimetry (DSC), and water vapour sorption isotherms. Finally, dissolution tests and
130 antioxidant activity measurements were performed *in vitro* to evaluate the enhancement of release
131 profiles and antioxidant activity of the quercetin SDs developed.

132 **2 Materials and methods**

133 **2.1 Materials**

134 Anhydrous quercetin (purity 99%) was obtained from Verbièse (France), polyethylene glycol with
135 molecular weights 1000 (PEG 1000) and 4000 g/mol (PEG 4000) was purchased from AcrosOrganics
136 (Belgium), and the PEG 6000 was supplied by Merck (Germany). Citric acid and 2,2-Diphenyl-1-
137 picrylhydrazyl (DPPH) was gifted from Sigma Aldrich (USA) and ethanol at 96% was supplied by
138 Carlo Erba Reagents (France). All the other materials and reagents were of analytical grade and purity.

139 **2.2 Equipment**

140 Quercetin-PEG solid dispersions were made by melt mixing in a high-speed disperser Dispermat®
141 LC55, equipped with a double jacket for heating and a temperature control system. A jacketed 50 ml
142 stainless-steel dispersion vessel (height = 50mm, inner diameter = 40mm) was used for batch charging.
143 Dispersion of quercetin was done with help of a stainless-steel disc (diameter = 3mm, thickness = 6mm).
144 The disc speed rotation could be varied from 0 to 20,000 tr/min.

145 **2.3 Preparation of quercetin-PEG physical mixture (PM) and solid dispersion (SD)**

146 A total weight of 10 g of quercetin-PEG SD with an amount of quercetin of 5, 20, 40, and 50% (w/w)
147 was prepared as follows. PEG polymer was placed in a vessel with the calculated amount of quercetin
148 powder, they were mixed at a selected impeller rotation speed of 10,000 rpm and melted at a specific
149 temperature (at 60°C for PEG 1000 and at 80 °C for PEG 4000 and PEG 6000) for 10 minutes. The
150 dispersion obtained was solidified at room temperature. The dispersion was transferred in a desiccator
151 for 24 h and then pulverised using a porcelain mortar and pestle. To obtain particles of uniform size, the
152 solid dispersions were crushed and then sieved (200µm). The resulting powder was stored in an airtight
153 container.

154 Physical mixtures with different mass amounts of quercetin (5, 20, 40 and 50%) were prepared by
155 mixing quercetin and PEG, using a mortar and pestle. The mixture obtained was sieved (200 μ m).

156 **2.4 X-ray diffraction analysis**

157 The powder's crystalline state was characterised using a Siemens D5000 X-Ray Powder Diffractometer.
158 This is a theta/theta2 diffraction instrument operating in reflection geometry using Fe K α radiation ($\lambda =$
159 1.54056 Å), which is focused on a Ge crystal primary monochromatic. The detector is a standard
160 scintillation counter. The scanning range for 2 θ was set at 10–45°, the step size was 0.025° with a
161 scanning rate of 0.5 step/s, and using an operating voltage and amperage set to 20.0 kV and 5.0 mA,
162 respectively. The K α 2 radiation of the copper was deleted with the software of the XRD. Experiments
163 were carried out on three replicates.

164 **2.5 Characterisation with FTIR spectroscopy**

165 Infrared spectra were obtained using an infrared spectrophotometer IR-TF Nicolet iS50 (Thermo
166 ScientificTM) in the wavenumber range of 400-4000 cm⁻¹ with the method of bromide pellets. 1 mg of
167 the sample was mixed with 8 mg of KBr in a mortar and pestle, the pellet was obtained by pressing the
168 previous melange in a press under 8T. Each experiment is reproduced three times.

169 **2.6 DSC measurement**

170 Heating curves of quercetin, PM, and SD were obtained using a differential scanning calorimeter (Q200
171 DSC, TA Instruments) equipped with a refrigeration unit. Samples (4–7 mg) were packed in a non-
172 hermetically crimped aluminium pan, and heated under dry nitrogen purge (50.0 ml/min). Samples were
173 heated from 25 °C to 400°C at 10 °C/min.

174 **2.7 Water vapour sorption measurement**

175 The dynamic water vapour sorption analyses, using a gravimetric dynamic sorption analyser SPS device
176 (SPS23, ProUmid GmbH & Co, Germany), were performed to investigate the moisture sorption
177 behaviour of pure compounds, SDs and PMs at 25°C. Samples (100-500mg) were poured into an
178 aluminium pan (50 mm diam. and 10 mm height) after first being dried at 0% RH at 25°C where the
179 equilibrium criterion for the drying step was 0.01% w/w change in 15min and a maximum drying time
180 of 60min. The samples were then exposed to constant relative humidity and temperature for known
181 periods of time. The sample was maintained at each RH until a plateau in the weight gain profile was
182 reached. All samples were maintained in a temperature and humidity-controlled chamber (\pm 0.6%) and
183 were sequentially weighed using a high precision microbalance (\pm 10 μ g). The analysis protocol and the
184 data exploitation were performed according to the literature (Afrassiabian & Saleh, 2020).

185 **2.8 Dissolution tests**

186 The dissolution profiles of pure quercetin, physical mixture (PM), and SDs were obtained in a buffer
187 solution (200 ml) of citric acid/NaOH at pH 5 at 100 rpm speed, at 37°C for 60 minutes, with quercetin
188 content fixed at 0.03 mg/ml. At time intervals (5, 10, 15, 20, 25, 30, 45, and 60 minutes), 1 ml of the
189 solution was collected, filtered (with a Whatman PP 0.45 μ m), and replaced with a clean solution.
190 Quercetin concentration was determined by spectrophotometer UV-Vis (Jasco V-530) at 370nm. All
191 measurements were repeated three times.

192 **2.9 In vitro antioxidant activity**

193 The antioxidant activity of quercetin, MP, and SD was measured using a 1,1-diphenyl-2-picrylhydrazyl

194 (DPPH) radical scavenging assay (Blois, 1958). The hydrogen atom donating ability of the quercetin
195 was determined by the discolouration of the ethanol solution of DPPH. DPPH produces a purple colour
196 in ethanol solution and fades to shades of yellow in the presence of antioxidants.

197 The quercetin-PEG samples were dissolved in ethanol to obtain a fixed concentration equivalent to IC50
198 of pure quercetin (0.3 µg/ml). 0.5µL of this solution was mixed with 1.5 mL of DPPH in ethanol
199 solution (0.024mg/mL). The blank sample was prepared with a similar procedure but without Que. The
200 reaction mixture was incubated in the dark at room temperature for 30 min. The activity was determined
201 by spectrophotometer UV-Vis (Jasco V-530) at 517 nm. Percentage of inhibition was calculated using
202 the following equation:

$$203 \quad \% \textit{Inhibition} = \frac{(A_{\textit{control}} - A_{\textit{sample}})}{A_{\textit{control}}} \quad (3)$$

204

205 where $A_{\textit{control}}$ is the absorbance of the control, and $A_{\textit{sample}}$ is the absorbance of the solid dispersion
206 sample. All the determinations were performed in triplicate.

207 **2.10 Determining solubility parameter δ**

208 The solubility parameter of quercetin was determined using the Hansen solubility parameters (HSPs)
209 approach (Hansen, 2007; S. Abbott, 2010), according to the experimental and numerical procedures
210 detailed in a previous paper (Imatoukene et al., 2020). A total of 32 organic solvents were tested in order
211 to classify them as adapted or non-adapted solvents. A mass of 30 mg of quercetin was placed in a glass
212 vial with 3 mL of the test solvent. The mixture was stirred vigorously and kept to rest for 24 h at room
213 temperature. The behaviour of the compounds was observed by visual inspection: a solvent was
214 considered a “good” or adapted solvent when the solute/solvent mixture formed a homogenous solution
215 (one-phase system), while a solvent was denoted a “bad” or non-adapted solvent when a two-phase
216 system was obtained. The HSPiP software (version 4.0.05 developed by Abbott and Yamamoto) was
217 used to calculate the HSP of quercetin. The solvents are coded in the programme with a number “1” for
218 soluble (one-phase system) or “0” for insoluble (two-phase system). Solvents, their solubility
219 parameters, and experimental scores were tabulated in **Table 1**.

220 Scores of the solubility tests were computed with HSPiP software providing the Hansen parameters of
221 quercetin and the radius of its solubility sphere by a quality-to-fit function. The coordinates of the
222 solubility volume centre were $\delta_d = 17.28 \text{ MPa}^{0.5}$, $\delta_p = 16.85 \text{ MPa}^{0.5}$ and $\delta_h = 11.97 \text{ MPa}^{0.5}$, while the
223 radius was $R_0 = 11.7 \text{ MPa}^{0.5}$. Therefore, the total solubility parameter δ was $26.9 \text{ MPa}^{0.5}$.

224 The solubility parameters for the polyethylene glycols (PEGs) were determined for the entire molecule
225 by the group contribution according to methods by Small (Small, 1953), Hoy (Hoy, 1985), and Van
226 Krevelen and Hoftyzer (D. W. Van Krevelen, 1976). The solubility parameters of polymers were
227 calculated, *inter alia*, from their molecular structure from the summation of the group molar attraction
228 constants divided by the molar volume of the polymer (Barton, 2017), taking into account the number of
229 monomer units and density. The prediction of quercetin-PEG miscibility was made using the free energy
230 of mixing (Eq. 1).

231 **Table 2** shows the solubility parameters obtained using group contributions methods, density (measured
232 by helium pycnometry), calculated molecular volumes and the Flory-Huggins interaction parameter.
233 This parameter was calculated from the solubility parameter obtained experimentally for quercetin and

234 those of the PEGs obtained by the three group contribution methods (Barton, 2017). The solubility
235 parameters calculated using the group molar attraction constants given by (Small, 1953) are much
236 smaller. Comparison of the values obtained with those obtained experimentally in the literature
237 (Sakellariou et al., 1986) showed that the methods of Hoy and of van Krevelen were acceptably close to
238 the experiment.

239 The values of χ were used for the construction of phase diagrams illustrating the variation of the total
240 free energy for the quercetin-PEG mixture as a function of the polymer volume fraction. The interaction
241 parameter was supposed independent of temperature.

242 **3 Results and Discussion**

243 **3.1 Predicting quercetin-PEG's miscibility**

244 In this work, the volume fraction of the quercetin and polymer were calculated by dividing the weight
245 fraction by the true density of the material, and the volume of the hypothetical lattice was defined as
246 being equal to the molecular volume of quercetin. The ratio of the PEG volume to that of the lattice site
247 was considered as the ratio of molar volumes of PEG and quercetin.

248 Using Eq. (1), the entropy of the mixture as a function of the polymer composition was predicted for the
249 quercetin-PEG systems, for three molecular weights of the polymer. The results were presented in **Fig.**
250 **1**. The effect of the different molecular weights M_w (between 1000 and 6000) of the polymer on the
251 thermodynamics of the mixture was weak (**Fig. 1-a**). Indeed, the entropy of the mixture with PEG 4000
252 and PEG 6000 is slightly less favourable than with PEG 1000. This can be explained by the
253 configurational entropy of the polymer, which was reduced due to the connectivity of the repeat units
254 (Marsac et al., 2006, 2009). The degree of contribution of entropy to the free energy term should
255 therefore have a relative effect. The miscibility would potentially be controlled by the enthalpy
256 interactions in the mixture and therefore by the difference between the solubility parameters of the
257 quercetin-PEG system.

258 **Fig. 1** (b, c and d) shows the evolution of the free energy of the mixture relative to the composition by
259 gradually increasing the volume fraction of the polymer in the quercetin-PEG binary mixture. According
260 to studies reported in the literature (Marsac et al., 2006, 2009; Shah et al., 2014; Thakral & Thakral,
261 2013), three categories of interactions were obtained depending on the group contributions method
262 employed for the PEG solubility parameter:

263 -The first category is characterised by obtaining a downward concave curve, the evolution of free energy
264 as a function of polymer composition, and a positive value of the total free energy of mixture predicting
265 immiscibility for all Quercetin-PEG systems, regardless of the value of the volume fraction of the
266 polymer in binary mixtures. In this case, the quercetin-PEG system tended to form a biphasic mixture
267 (**Fig. 1-b**).

268 - The second is represented by a downward concave curve followed by a concave free energy ascending
269 curve of the mixture with respect to the composition by gradually increasing the volume fraction of the
270 polymer in the binary mixture. The total free energy of the mixture for compositions containing a small
271 proportion of polymer was positive, its value became negative when the polymer fraction increased
272 beyond 60%. The findings indicated that the quercetin-PEG mixture tends to form a biphasic system
273 with a low concentration of the polymer, but the binary system should exhibit a single phase when

274 increasing the fraction of polymer (**Fig. 1-b, c**).

275 -The third was only observed in the case of the quercetin-PEG1000 mixture using the contribution
276 groups method of van Krevelen, which gives negative values of the total free energy of mixing and an
277 overall concave upward shape of the free energy curve (**Fig. 1-c**). The low positive value of the
278 enthalpic contribution, in this case, appears to be counterbalanced by the total increase in system entropy
279 and, therefore, the system exhibits negative free energy mixing for all proportions of quercetin and
280 PEG1000. In this particular case, quercetin can be considered miscible with PEG 1000 in all
281 proportions. It is believed that the interacting adhesive forces between quercetin and PEG1000 are
282 thought to be stronger than the cohesive forces and therefore facilitate mixing, leading to the probable
283 formation of solid solution or the crystallization of quercetin at the amorphous state. Moreover, for the
284 PEG 4000 and PEG 6000, the entropy of the system could not counterbalance the low positive value of
285 the enthalpy, but it did contribute to reducing the total free energy of the system to values relatively
286 close to zero.

287 Taking into account the study that had shown that the methods of Hoy, and of van Krevelen and Hoy,
288 provided PEG solubility parameter values closest to the experimental values (Sakellariou et al., 1986),
289 estimating the free energy of mixing predicts that the miscibility of the quercetin-PEG system would
290 decrease with the increase in PEG molecular weight and in volume fraction polymer. It should be noted
291 that the contribution of the enthalpy of the mixture was estimated from the solubility parameters of
292 quercetin and PEGs at a temperature of 25°C. Therefore, it can be expected that a system that is
293 immiscible at low temperatures can achieve miscibility at a higher temperature; without forgetting the
294 considerable contribution of the mixing process, which generates a significant shear force in the media
295 and consequently improves miscibility.

296 **3.2 X-Ray diffraction**

297 The diffractogram of the pure compounds (**Fig. 2**) showed that the different grades of polymers used,
298 PEG1000, PEG 4000 and PEG 6000, had the same semi-crystalline structure demonstrated by two
299 significant peaks at 19.68° and 23.85° in 2 θ (Baird et al., 2010), while quercetin had the peaks at 14.47°,
300 26.89°, 27.67° and 28.65° in 2 θ (Gilley et al., 2017). Thus, given the fact that the crystal structures of
301 quercetin differed from PEGs, it was possible to determine the presence of crystalline quercetin within
302 the solid dispersions (SD). The physical mixtures (PM) with an amount of quercetin of 40% (w/w) were
303 also characterised to compare.

304 For all physical mixtures, a low presence of crystalline quercetin via its peak at 14.47°, synonymous
305 with the crystalline structure of quercetin in the crystalline matrix, could be observed, while for SD1
306 (quercetin-PEG 1000), SD4 (quercetin-PEG 4000), and SD6 (quercetin-PEG 6000), containing a
307 quercetin mass composition up to 40% (w/w), the presence of crystalline quercetin was no longer
308 observed. The quercetin peaks intensity in the samples was significantly less than that of pure quercetin.
309 In this case, the state of amorphous quercetin in the precipitated form in the crystalline matrix can be
310 suggested. Moreover, in the case of SD1 40% (w/w), the absence of the characteristic peaks of the
311 crystalline state was observed, not only for quercetin but also for PEG 1000 which becomes relatively
312 amorphous after cooling the formulation, forming an amorphous solid dispersion. This is explained by
313 the favourable molecular interactions, predicted by the free energy of the mixture between quercetin and
314 PEG, and their mutual roles as crystallization inhibitors which become noticeable in the solid

315 dispersions SD1 40% compared to this class of low molecular weight PEG. However, the diffractogram
316 of all SDs with a quercetin content of 50% (w/w) revealed the crystalline structure of quercetin. On the
317 other hand, in the case of SD1, recrystallization of PEG 1000 was inhibited by quercetin.

318 In the following steps, for better evaluation and understanding of the effect of molecular weight on the
319 properties of quercetin, the characterisation results of solid dispersions at 40% (w/w) will be developed
320 and discussed.

321 **3.3 Thermal behaviour**

322 Solid dispersions, as well as physical mixtures containing 40% (w/w) of quercetin, were characterised
323 and compared by thermal analysis. The thermograms of binary mixtures containing quercetin and
324 different grades of PEG are shown in **Fig. 3**. Quercetin was characterised by an endothermic melting
325 peak around 330°C and an exothermic peak near 344°C, which refers to its decomposition (De Mello
326 Costa et al., 2011). The endothermic-melting peak for PEGs occurs at 35.60, 61.7, and 67°C for PEG
327 1000, PEG 4000, and PEG 6000 respectively.

328 In the case of physical mixtures (PM), **Fig. 3** shows the absence of a fusion endotherm for quercetin.
329 The results correspond to only one peak at the melting of the polymer in the binary mixture. The non-
330 appearance of the endothermic peak of quercetin in PM was observed in the literature (Khan et al., 2011;
331 Thakral & Thakral, 2013) where analysis of samples containing 20%–40% (w/w) of pharmaceutical
332 drugs in the presence of PEG 8000 and PEG 6000 showed only a single peak corresponding to the
333 melting of the polymer. It has been proposed that during the heating process for analysis, especially if
334 the difference in melting point is significant (as the case here between PEGs and quercetin), the molten
335 carrier begins to solubilize the drug by thus dispersing it in its matrix; with the consequence that the
336 drug endotherm completely disappears. The results obtained for the binary physical mixtures also
337 detected that there was sufficient physical interaction between the components leading to the lowering of
338 the melting point of the polymers to 28.5, 60.25, and 62.23 °C for PEG 1000, PEG 4000, and PEG 6000
339 respectively.

340 In the case of solid dispersions, for PEG 4000 and PEG 6000, the physical interactions were stronger,
341 resulting in a lowering of the melting point to 58.70 and 60.41°C for PEG 4000 and PEG 6000
342 respectively. In the case of the quercetin-PEG1000 mixture, we observed the absence of a melting peak
343 for quercetin and the polymer. This can be considered synonymous with the strong miscibility of
344 quercetin with PEG 1000 on the one hand, and with the inhibition of the recrystallization of PEG 1000
345 in the presence of quercetin in the binary mixture, upon cooling of the solid dispersion in process. These
346 results concur with those obtained by DRX analysis and predicted by the mixing free energy model
347 using the van Krevelen method to calculate the Flory interaction parameter. The latter predicted total
348 miscibility in the binary quercetin-PEG 1000 mixture, resulting in a strong adhesive interaction between
349 the two constituents compared to the cohesive interactions of each component. All these results confirm
350 that quercetin forms an amorphous solid dispersion with crystalline matrixes PEG 4000 and PEG 6000,
351 and a glass solution with amorphous PEG 1000 where the quercetin molecules were dissolved or
352 molecularly dispersed with the amorphous matrix.

353 **3.4 Fourier transform infrared spectroscopy**

354 Further evidence for intermolecular interactions in solid dispersions has been obtained by means of
355 infrared spectroscopic examination. FTIR has been used to explore quercetin-polymer interactions in

356 SD. IR spectra of quercetin, PEGs, quercetin-PEG (40% w/w) physical mixtures, and solid dispersions
357 are shown in **Fig. 4**. Quercetin and PEG FTIR peaks were found in accordance with those reported in the
358 literature (Dwi et al., 2018; Indra et al., 2020).

359 The comparison of the infrared spectra of the pure compounds and the mixtures shows the absence of
360 the creation of covalent bonds between the two compounds in the mixture and that they were not
361 degraded during mixing. No clear changes in vibration bands were observed in quercetin with PEGs. In
362 fact, it was the most readable function for seeing if there had been a modification to the hydrogen bonds.
363 To estimate the creation of hydrogen bonds between PEG and quercetin allowing the mixture to be
364 stabilized, the functional group of quercetin studied was C=O (1670 cm^{-1}). The study of the
365 characteristic band C=O made it possible to confirm the creation of intermolecular H bonds. In the solid
366 dispersions, a significant displacement of this band was observed toward 1652 , 1653 , and 1654 cm^{-1} for
367 PEG 1000, PEG 4000, and PEG 6000 respectively, while this was not observed in the physical mixtures
368 (**Fig. 5**). This shift in the wavenumber of infrared spectra is synonymous with physical interactions
369 caused by weak interactions, such as hydrogen bond interactions between functional groups of quercetin
370 and PEG. A hydrogen bond between the carbonyl group of quercetin and the terminal hydroxyl group of
371 PEGs is quite possible. Moreover, peaks were barely visible around 3300 and 3400 cm^{-1} on the spectra
372 of SD4 and SD6 (**Fig. 4**), indicating that quercetin was only partially amorphous in these solid
373 dispersions (Gilley et al., 2017), in agreement with the DRX analysis (**Fig. 2**).

374 **3.5 Moisture sorption isotherms**

375 A water sorption isotherm at 25°C was used to evaluate the effect of the PEG Mw carrier on quercetin-
376 PEG solid dispersions and their physical stability. PEG is a hygroscopic and semi-crystalline material
377 and can undergo deliquescence. Deliquescence is a process by which highly water-soluble crystalline or
378 semi-crystalline materials undergo a solid-to-solution phase transformation through sorption of large
379 quantities of atmospheric moisture (Dupas-Langlet et al., 2017). The sorption of large amounts of
380 moisture by solid dispersions can potentially have an impact not only on phase behaviour, but also on
381 chemical and physical stability, as well as microbiological properties.

382 Moisture sorption isotherms for pure quercetin, various PEGs, PMs, and SDs were measured at 25°C
383 between 0 to 85 % RH (**Fig. 6**). Quercetin presented slight moisture sorption of about 2.54 % (w/w) at
384 85% RH and 25°C , a low uptake level due to surface adsorption, while the PEG isotherms were
385 characterised by a sharp increase in moisture content depending on the contribution of both adsorption
386 and absorption phenomena. In addition to surface sorption, it is widely accepted that semi-crystalline
387 polymers will also sorb moisture into the amorphous region at the lower RH (Schachter et al., 2004).
388 **Fig. 6** a,b and c shows that water content remains negligible (<1%) up to approximately 30, 60, and
389 65% RH, then a relatively gradual increase in the water content of the polymers, and finally, at higher
390 RH, an increase of water uptake up to 76, 30 and 16% for pure PEG 6000, PEG 4000, and PEG 6000
391 respectively. Moreover, the inflexion point corresponding to the deliquescence phenomenon of
392 crystalline PEGs, characterised by an intense increase in water content, was observed at a different RH
393 for each grade. The deliquescence relative humidity (RH_0) for PEG 1000, PEG 4000, and PEG 6000,
394 measured by extrapolating the linear parts of the vapour sorption isotherm before and after the
395 deliquescence, was estimated at 54, 77, and 79 % RH, respectively. The values obtained were very close
396 to those reported in the literature (Baird et al., 2010).

397 PEG can form numerous hydrogen bonds with water through the functional molecular groups of ether
398 oxygen atoms (–O–) in the oxyethylene polymer backbone and hydroxyl (-OH) end groups. The
399 decrease in water uptake, with polymer molecular weight, can be explained by the fact that the relative
400 fraction of the hydroxyl end groups decreases, hence the higher molecular weight grades are less
401 hydrophilic and will have lower water affinity.

402 The findings have also been explained in the literature by the fact that at low RH, solid PEG crystallizes,
403 obstructing the penetration of water molecules to access oxygen atoms in the PEG chains and thus the
404 water uptake (Thijs et al., 2007). At high RH, it was proposed that when a first hydration shell is formed
405 in the PEG, the PEG chains would adapt the desired conformation or arrangement of the polymer chains
406 to be able to form extensive hydrogen bonds with water, favouring the uptake of more water. The results
407 obtained here obey this proposed mechanism and show that the decrease in the molecular weight of PEG
408 favours those mechanisms for water absorption.

409 The hydrophobic character and non-deliquescence of pure quercetin were demonstrated by the low
410 sorption of water (2% at 85% RH) in **Fig. 6**. In contrast, the water uptake in solid dispersion SD1
411 increased to 47% at 85% RH, while those of SD4 and SD6 increased to 30 and 18% respectively. The
412 PMs show a nearly identical sorption isotherm as the solid dispersion.

413 In other words, the addition of quercetin at 40% (w/w) had a minimal effect on the moisture sorption
414 behaviour of PEG 4000 and PEG 6000, which allocated to the presence of quercetin amorphous
415 precipitates in the crystalline matrix. However, just before the deliquescence relative humidity (HR₀
416 =77%) of PEG 4000, a moderate increase in water uptake could be observed which was attributed to the
417 new molecular arrangement which helps access certain polar functional groups in solid dispersion.

418 Moreover, compared to PEG 1000 moisture sorption, the SD1 data show a decrease in water sorption at
419 high RH in the presence of hydrophobic molecules of quercetin. These latter obstructed the functional
420 groups in solid dispersion, by means of the steric effect, by making them unavailable to interact with
421 water during sorption. To confirm that, the interaction between quercetin and PEGs was evaluated using
422 the deviation of SD1 water uptake from the ideal behaviour theoretically predicted. The theoretical
423 moisture gain, supposing no interaction between the components, was estimated by summation of the
424 moisture sorption profiles of the two individual components with respect to their mass fractions
425 (Crowley & Zografi, 2002). It is stated in the literature that theoretical moisture gain is valid for a model
426 binary system of two miscible amorphous components. A deviation in the amount of water taken up
427 could be observed for all cases as represented in **Fig. 6**. A decrease in the amount of water taken up in
428 melt mixing SD1 could particularly be noted, which confirmed the relatively strong interaction of
429 quercetin and PEG 1000 and the amorphous structure of SD1, as already indicated.

430 **3.6 Quercetin release profiles**

431 The quercetin dissolution profiles of pure quercetin, PMS and SDs are presented in **Fig. 7**. The
432 dissolution studies were conducted only on SDs and PMs prepared with 40% w/w, to understand the
433 effect of completely amorphous and crystalline systems on dissolution. In this study, the dissolution
434 efficiency of minute 30 (DE30) was selected to compare the quercetin release rate in solid dispersion,
435 under non-sink conditions and without added surfactant. The result was compared to that of pure
436 crystalline quercetin under similar conditions.

437 The DE30 of quercetin, PM1, PM4, and PM6 was 1.64, 1.78, 1.78, and 0.98% respectively; while for

438 SD1, SD4 and SD6, the DE30 was 7.71, 3.46, and 6.05 %. The solubility of quercetin in the medium
439 was very low, it was solubilized after only 10 minutes to reach a maximum value (1.6 %). Compared to
440 pure quercetin, all PMs showed relatively faster dissolution during the first 10 minutes, and then it did
441 not result in any change in the dissolution profile and solubility, according to XRD data where no
442 changes in the crystal structure of quercetin were observed in PMs.

443 All three PEG matrices displayed similarly low quercetin release (<10%), while still much faster and
444 more complete than pure quercetin and the physical mixture. Some results were obtained in the works of
445 Gilley (Gilley et al., 2017), concerning the solid dispersion of quercetin in cellulose derivate matrices
446 (quercetin/cellulose derivate=1/9, pH=6.8), using spray-dried process; it was found within 30 min,
447 quercetin release reached 13–14% then decreased rapidly to 4–5% within 5h. To enhance the dissolution
448 and bioavailability of quercetin, a novel blend of cellulose derivate matrices with hydrophilic PVP was
449 proposed (Gilley et al., 2017).

450 **Fig. 7** shows the increase in the dissolution rates of quercetin in solid dispersion SDs, compared to PMs
451 and pure quercetin, which may be due to the amorphous state of quercetin in a polymeric matrix (Shah
452 et al., 2014). The hydrophilic polymer encapsulated the hydrophobic compound and helped to solubilize
453 the compound readily due to its rapid contact with the dissolution media (Alshehri et al., 2020).
454 Moreover, the SD1 formulation prepared with PEG1000 showed that quercetin release was very rapid.
455 At 5 minutes of dissolution, more than 7.30 % of the quercetin had dissolved from solid dispersion SD1,
456 whereas SD4 and SD6 dissolved 2.17 and 4.30 % respectively.

457 These results were attributed to the amorphous solid dispersion of SD1, according to XRD and DSC
458 data, where the quercetin was molecularly dispersed with the amorphous matrix. Molecules present in a
459 random arrangement in the amorphous state offered a lower thermodynamic barrier to dissolution and
460 superior molecular motion that made possible a faster dissolution rate. Consequently, the amorphous
461 form showed higher solubility, a higher rate of dissolution, and then better bioavailability than the
462 crystalline structure.

463 **3.7 Antioxidant activity**

464 The 2,2-diphenyl-1-picrylhydrazyl (DPPH) radical scavenging activities of quercetin and solid
465 dispersions (SD1, SD4 and SD6) with a fixed mass ratio (40%) were evaluated. The results are
466 illustrated in the **Fig. 8**. Determining the antioxidant activity of the solid dispersions made it possible to
467 determine the impact of the formulation on this property because all the samples had the same amount of
468 quercetin. The results obtained showed an increase in the anti-radical activity of the different solid
469 dispersions compared to pure quercetin (49.22% ± 3.01). These results obtained show a slight effect of
470 PEG grade on the antioxidant activity.

471 The significant result of higher antioxidant activity was achieved due to the greater improvement in
472 solubility and dissolution due to the amorphization of quercetin by melt mixing compared to the
473 physical mixtures. Of the three SDs prepared, the highest DPPH radical scavenging activity was
474 achieved by SD6 (76.61% ± 4.06), followed by SD4 (74.60% ± 3.50) and then by SD1 (68.70% ± 3.06).
475 Although characterising SD1 at 40% quercetin revealed the formation of amorphous solid dispersion,
476 the latter did not show superior anti-radical activity compared to other SDs. The results of the study
477 revealed that quercetin-PEG solid dispersions formation showed good radical scavenging activity and
478 antioxidant activities compared to pure quercetin. Statistical analysis using the one-way analysis of

479 variance confirmed this (p-value < 0.05). The fact that antioxidant activity increased may stem from the
480 better availability of the alcoholic protons of quercetin (or electron e-donation) in the solution that can
481 convert DPPH into DPPH-H. The amorphous state of quercetin was found in several polymeric
482 matrices, which, in the absence of organisation, made possible better availability of antioxidant protons.

483 **4 Conclusion**

484 The quercetin SD formulations were prepared using the melt mixing or fusion method in a high-speed
485 disperser process using PEG 1000, 4000 and 6000 as the hydrophilic matrix to enhance the dissolution
486 rate and antioxidant activity of quercetin.

487 The theoretical estimation of total Gibbs free energy and Flory-Hugging interaction parameters for
488 quercetin with various molecular weights of PEG was performed using the solubility parameters. This
489 last was experimentally determined using the Hansen solubility parameter method for quercetin while
490 that of PEGs was calculated using the group contribution methods. Thus, it was possible to produce a
491 total Gibbs free energy diagram of the system versus volume fraction polymer in a binary mixture. In
492 this study, Van Krevelen and Hoftyzer's group contribution methods gave a good prediction of
493 interaction and miscibility behaviour, particularly between quercetin and PEG 1000. The theoretical
494 estimation of free energy predicted a decrease in miscibility with the increase in molecular weight of the
495 PEG. The results of X-ray diffraction and differential scanning calorimetry of the dispersion solid, with
496 40% (w/w) of quercetin, revealed a structure transformation from crystalline to the amorphous state of
497 quercetin in all SDs. Moreover, an amorphous solid dispersion or glassy solution was formed, between
498 quercetin and PEG 1000, with a mutual role as a crystallization inhibitor. The IR study spectra revealed
499 a weak physical interaction involving hydrogen bonds between the quercetin molecules and the polymer
500 chains of PEGs. Moreover, characterising the interaction and stability of quercetin-PEG SDs using DVS
501 made it possible to confirm the presence of quercetin amorphous precipitates in the crystalline matrix of
502 PEG 4000 and PEG 6000, and the amorphous structure of SD1 with low water uptake and relatively
503 strong interaction of quercetin and PEG. The result of this study reveals low enhancement in the
504 dissolution rate of quercetin from all SDs. The amorphous SD1 showed a higher rate of dissolution,
505 about 10%. However, that is still much faster and more complete compared to the release of pure
506 quercetin and physical mixture (<1.6%). All the SD formulations achieved good antioxidant and/or
507 activity radical scavenging generated by the amorphous state of quercetin in the PEG polymer matrix.

508

509 **Acknowledgements**

510 We thank Region Hauts-de-France for the financial support of the Valantiox project. Valantiox project
511 aims to enhance the antioxidant potential of low-water solubility polyphenols, by formulating solid
512 dispersions to improve their bioavailability.

513

514 **References**

515

- 516 Afrassiabian, Z., & Saleh, K. (2020). Caking of anhydrous lactose powder owing to phase transition and
517 solid-state hydration under humid conditions: From microscopic to bulk behavior. *Powder*
518 *Technology*, *363*, 488–499. <https://doi.org/10.1016/j.powtec.2020.01.033>
- 519 Alshehri, S., Sarim, S., Altamimi, M. A., Hussain, A., Shakeel, F., Elzayat, E., Mohsin, K., Ibrahim, M.,
520 & Alanazi, F. (2020). *Enhanced Dissolution of Luteolin by Solid Dispersion Prepared by Different*
521 *Methods: Physicochemical Characterization and Antioxidant Activity*.
522 <https://doi.org/10.1021/acsomega.9b04075>
- 523 Baird, J. A., Olayo-Valles, R., Rinaldi, C., & Taylor, L. S. (2010). Effect of Molecular Weight,
524 Temperature, and Additives on the Moisture Sorption Properties of Polyethylene Glycol. *Journal of*
525 *Pharmaceutical Sciences*, *99*(1), 154–168. <https://doi.org/10.1002/jps.21808>
- 526 Baird, J. A., & Taylor, L. S. (2012). Evaluation of amorphous solid dispersion properties using thermal
527 analysis techniques. *Advanced Drug Delivery Reviews*, *64*(5), 396–421.
528 <https://doi.org/10.1016/j.addr.2011.07.009>
- 529 Barton, A. F. M. (2017). *CRC Handbook of Solubility Parameters and Other Cohesion Parameters*.
530 Routledge. <https://doi.org/10.1201/9781315140575>
- 531 BLOIS, M. S. (1958). Antioxidant Determinations by the Use of a Stable Free Radical. *Nature*,
532 *181*(4617), 1199–1200. <https://doi.org/10.1038/1811199a0>
- 533 Chow, V. T., Manuel, R., Biancatelli, L. C., Colunga Biancatelli, L., Berrill, M., Catravas, J. D., &
534 Marik, P. E. (2020). Quercetin and Vitamin C: An Experimental, Synergistic Therapy for the
535 Prevention and Treatment of SARS-CoV-2 Related Disease (COVID-19). *Frontiers in Immunology*
536 | *Www.Frontiersin.Org*, *1*, 1451. <https://doi.org/10.3389/fimmu.2020.01451>
- 537 Crowley, K. J., & Zografi, G. (2002). Water Vapor Absorption into Amorphous Hydrophobic
538 Drug/Poly(vinylpyrrolidone) Dispersions. *Journal of Pharmaceutical Sciences*, *91*(10), 2150–2165.
539 <https://doi.org/10.1002/jps.10205>
- 540 de Mello Costa, A. R., Marquiasfável, F. S., de Oliveira Lima Leite Vaz, M. M., Rocha, B. A., Pires
541 Bueno, P. C., Amaral, P. L. M., da Silva Barud, H., & Berreta-Silva, A. A. (2011). Quercetin-PVP
542 K25 solid dispersions : Preparation, thermal characterization and antioxidant activity. *Journal of*
543 *Thermal Analysis and Calorimetry*, *104*(1), 273–278. <https://doi.org/10.1007/s10973-010-1083-3>
- 544 Dupas-Langlet, M., Benali, M., Pezron, I., & Saleh, K. (2017). Characterization of saturated solutions
545 and establishment of “aw-phase diagram” of ternary aqueous inorganic-organic and organic-
546 organic systems. *Journal of Food Engineering*, *201*, 42–48.
547 <https://doi.org/10.1016/j.jfoodeng.2017.01.009>
- 548 Dwi, S., Febrianti, S., Zainul, A., & Retno, S. (2018). PEG 8000 increases solubility and dissolution rate
549 of quercetin in solid dispersion system. *Marmara Pharmaceutical Journal*, *22*(2), 259–266.
550 <https://doi.org/10.12991/mpj.2018.63>

551 D. W. Van Krevelen. (1976). *Properties of polymers, their estimation and correlation with chemical*
552 *structure – (2nd rev. ed.)*, D. W. Van Krevelen, Elsevier, Amsterdam – Oxford – New York, 1976,
553 620 pp. (E. M. Pearce, Ed.; 2nd ed.). <https://doi.org/10.1002/pol.1977.130150109>

554 El-Saber Batiha, G., Magdy Beshbishy, A., Ikram, M., Mulla, Z. S., Abd El-Hack, M. E., Taha, A. E.,
555 Algammal, A. M., Hosny, Y., & Elewa, A. (2020). *The Pharmacological Activity, Biochemical*
556 *Properties, and Pharmacokinetics of the Major Natural Polyphenolic Flavonoid: Quercetin*. 9,
557 374. <https://doi.org/10.3390/foods9030374>

558 Gilley, A. D., Arca, H. C., Nichols, B. L. B., Mosquera-Giraldo, L. I., Taylor, L. S., Edgar, K. J., &
559 Neilson, A. P. (2017). Novel cellulose-based amorphous solid dispersions enhance quercetin
560 solution concentrations in vitro. *Carbohydrate Polymers*, 157, 86–93.
561 <https://doi.org/10.1016/j.carbpol.2016.09.067>

562 Hansen, C. M. (2007). *Hansen Solubility Parameters*. CRC Press.
563 <https://doi.org/10.1201/9781420006834>

564 HOY, K. L. (1985). The Hoy tables of solubility parameters. *Union Carbide Corporation, Solvents &*
565 *Coatings Materials, Research & Development Department*.

566 Imatoukene, N., Koubaa, M., Perdrix, E., Benali, M., & Vorobiev, E. (2020). Combination of cell
567 disruption technologies for lipid recovery from dry and wet biomass of *Yarrowia lipolytica* and
568 using green solvents. *Process Biochemistry*, 90, 139–147.
569 <https://doi.org/10.1016/J.PROCBIO.2019.11.011>

570 Indra, P., Zaini, E., Ismed, F., & Lucida, H. (2020). Preparation and characterization of quercetin-
571 polyvinylpyrrolidone K-30 spray dried solid dispersion [Preparación y caracterización de
572 dispersión sólida de quercetina-polivinilpirrolidona K-30 secada por rociado]. *Journal of Pharmacy*
573 *& Pharmacognosy Research*, 8(2), 127–134. <http://jppres.com/jppres>

574 Kanaze, F. I., Kokkalou, E., Niopas, I., Georgarakis, M., Stergiou, A., & Bikiaris, D. (2006). Dissolution
575 enhancement of flavonoids by solid dispersion in PVP and PEG matrixes: A comparative study.
576 *Journal of Applied Polymer Science*, 102(1), 460–471. <https://doi.org/10.1002/app.24200>

577 Khalid, N., Kobayashi, I., Neves, M. A., Uemura, K., Nakajima, M., & Nabetani, H. (2016).
578 Microchannel emulsification study on formulation and stability characterization of monodisperse
579 oil-in-water emulsions encapsulating quercetin. *Food Chemistry*, 212, 27–34.
580 <https://doi.org/10.1016/j.foodchem.2016.05.154>

581 Li, B., Konecke, S., Harich, K., Wegiel, L., Taylor, L. S., & Edgar, K. J. (2013). Solid dispersion of
582 quercetin in cellulose derivative matrices influences both solubility and stability. *Carbohydrate*
583 *Polymers*, 92(2), 2033–2040. <https://doi.org/10.1016/j.carbpol.2012.11.073>

584 Manca, M. L., Lai, F., Pireddu, R., Valenti, D., Schlich, M., Pini, E., Ailuno, G., Fadda, A. M., &
585 Sinico, C. (2020). Impact of nanosizing on dermal delivery and antioxidant activity of quercetin
586 nanocrystals. In *Journal of Drug Delivery Science and Technology* (Vol. 55). Editions de Sante.
587 <https://doi.org/10.1016/j.jddst.2019.101482>

588 Marsac, P. J., Li, T., & Taylor, L. S. (2009). Estimation of drug-polymer miscibility and solubility in
589 amorphous solid dispersions using experimentally determined interaction parameters.
590 *Pharmaceutical Research*, 26(1), 139–151. <https://doi.org/10.1007/s11095-008-9721-1>

591 Marsac, P. J., Shamblin, S. L., & Taylor, L. S. (2006). Theoretical and practical approaches for
592 prediction of drug-polymer miscibility and solubility. *Pharmaceutical Research*, 23(10), 2417–

593 2426. <https://doi.org/10.1007/s11095-006-9063-9>

594 S. Abbott, C. M. H. H. Y. (2010). *Hansen Solubility Parameters in Practice* (Hansen-Solubility.com,
595 Ed.; 5th ed.).

596 Sakellariou, P., Rowe, R. C., & White, E. F. T. (1986). The solubility parameters of some cellulose
597 derivatives and polyethylene glycols used in tablet film coating. *International Journal of*
598 *Pharmaceutics*, *31*(1–2), 175–177. [https://doi.org/10.1016/0378-5173\(86\)90229-2](https://doi.org/10.1016/0378-5173(86)90229-2)

599 Schachter, D. M., Xiong, J., & Tirol, G. C. (2004). Solid state NMR perspective of drug–polymer solid
600 solutions: a model system based on poly(ethylene oxide). *International Journal of Pharmaceutics*,
601 *281*(1–2), 89–101. <https://doi.org/10.1016/j.ijpharm.2004.05.024>

602 Shah, N., Sandhu, H., Choi, D. S., Chokshi, H., & Malick, A. W. (Eds.). (2014). *Amorphous Solid*
603 *Dispersions*. Springer New York. <https://doi.org/10.1007/978-1-4939-1598-9>

604 Small, P. A. (1953). Some factors affecting the solubility of polymers. *Journal of Applied Chemistry*,
605 *3*(2), 71–80. <https://doi.org/10.1002/jctb.5010030205>

606 Thakral, S., & Thakral, N. K. (2013). Prediction of drug-polymer miscibility through the use of
607 solubility parameter based flory-huggins interaction parameter and the experimental validation:
608 PEG as model polymer. *Journal of Pharmaceutical Sciences*, *102*(7), 2254–2263.
609 <https://doi.org/10.1002/jps.23583>

610 Thijs, H. M. L., Becer, C. R., Guerrero-Sanchez, C., Fournier, D., Hoogenboom, R., & Schubert, U. S.
611 (2007). Water uptake of hydrophilic polymers determined by a thermal gravimetric analyzer with a
612 controlled humidity chamber. *Journal of Materials Chemistry*, *17*(46), 4864.
613 <https://doi.org/10.1039/b711990a>

614 Ulrich, R. D. (1978). P. J. Flory. In *Macromolecular Science* (pp. 69–98). Springer US.
615 https://doi.org/10.1007/978-1-4684-2853-7_5

616 Yang, S. L., Zhao, L. J., Chi, S. M., Du, J. J., Ruan, Q., Xiao, P. L., & Zhao, Y. (2019). Inclusion
617 complexes of flavonoids with propylenediamine modified β -cyclodextrin: Preparation,
618 characterization and antioxidant. *Journal of Molecular Structure*, *1183*, 118–125.
619 <https://doi.org/10.1016/J.MOLSTRUC.2019.01.046>

620 Zou, Y., Qian, Y., Rong, X., Cao, K., McClements, D. J., & Hu, K. (2021). Encapsulation of quercetin
621 in biopolymer-coated zein nanoparticles: Formation, stability, antioxidant capacity, and
622 bioaccessibility. *Food Hydrocolloids*, *120*, 106980.
623 <https://doi.org/10.1016/J.FOODHYD.2021.106980>

624
625
626

627
628
629

630 **Table 1**

631 Solvents classification used to solubilize quercetin and the determination of the Hansen solubility
632 parameters (Fit= 1.000, Wrong In= 0, Wrong Out= 0). Solubility parameters were taken from the
633 literature (Hansen, 2007) or predicted using the Yamamoto Molecular Break (Y-MB) group-contribution
634 method (S. Abbott, 2010).

Solvent	δ_D	δ_P	δ_H	Score
Hexane	14.9	0	0	0
Pentane	14.5	0	0	0
Decane	15.7	0	0	0
Heptane	15.3	0	0	0
Ethyl Benzene	17.8	0.6	1.4	0
Toluene	18	1.4	2	0
Chloroform	17.8	3.1	5.7	0
1-Decanol	16	4.7	10.5	0
1-Octanol	16	5	11.2	0
2-Methyl-1-Butanol	16	5.1	14.3	0
Ethyl Acetate	15.8	5.3	7.2	0
2-Butanol	15.8	5.7	14.5	0
Aniline	20.1	5.8	11.2	0
3-Methyl Allyl Alcohol	16	6	15.5	1
1-Propanol	16	6.8	17.4	0
Ethanol	15.8	8.8	19.4	1
Formic Acid	14.6	10	14	1
Acetone	15.5	10.4	7	1
Allyl Alcohol	16.2	10.8	16.8	1
Ethylene Glycol	17	11	26	0
Methanol	14.7	12.3	22.3	0
Triethylene Glycol	16	12.5	18.6	1
Diethyl Sulfate	15.7	12.7	5.1	1
Dimethyl Formamide (DMF)	17.4	13.7	11.3	1
Formaldehyde	12.8	14.4	15.4	1
Ethanolamine	17	15.5	21	1
Nitroethane	16	15.5	4.5	1
Water	15.5	16	42.3	0
Dimethyl Sulfoxide (DMSO)	18.4	16.4	10.2	1
Propylene Carbonate	20	18	4.1	1
Nitromethane	15.8	18.8	6.1	1
Formamide	17.2	26.2	19	1

635

636

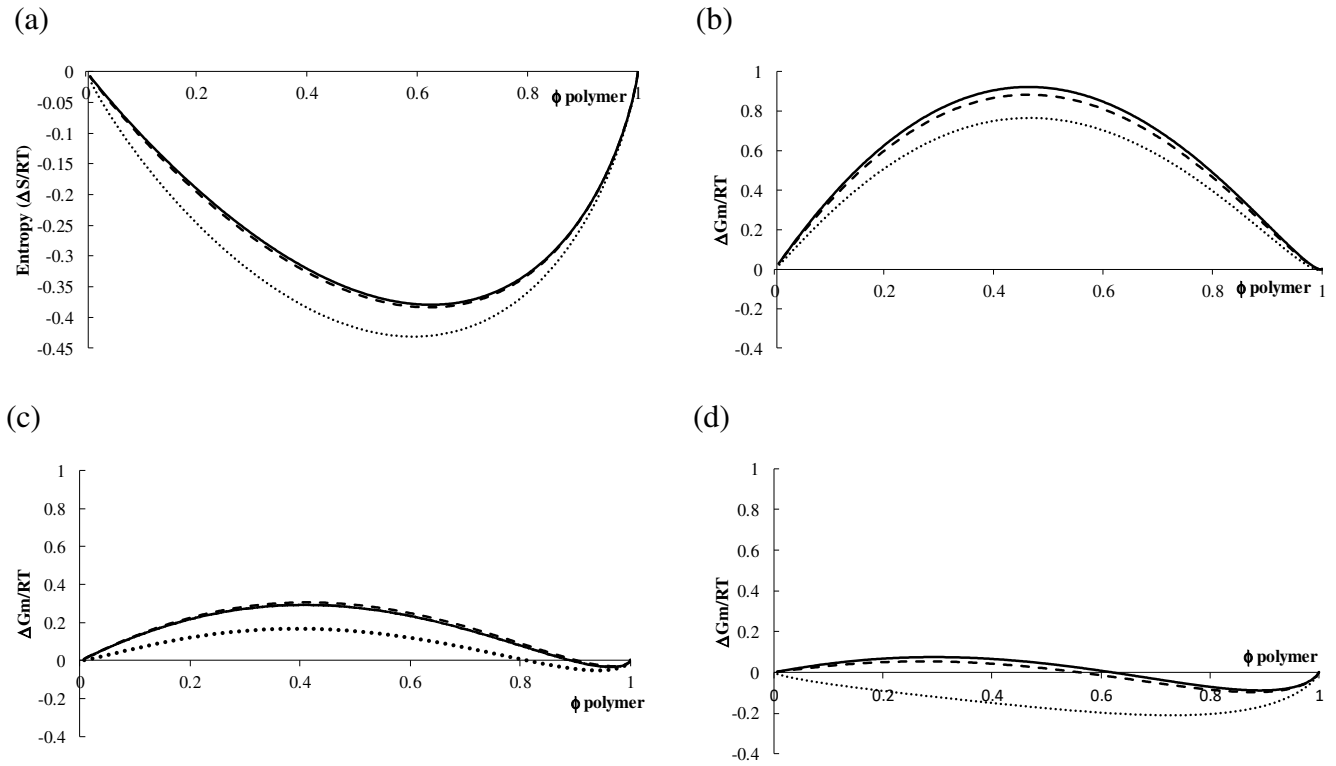
637 **Table 2**

638 PEGs and quercetin properties used to calculate the free energy of mixing

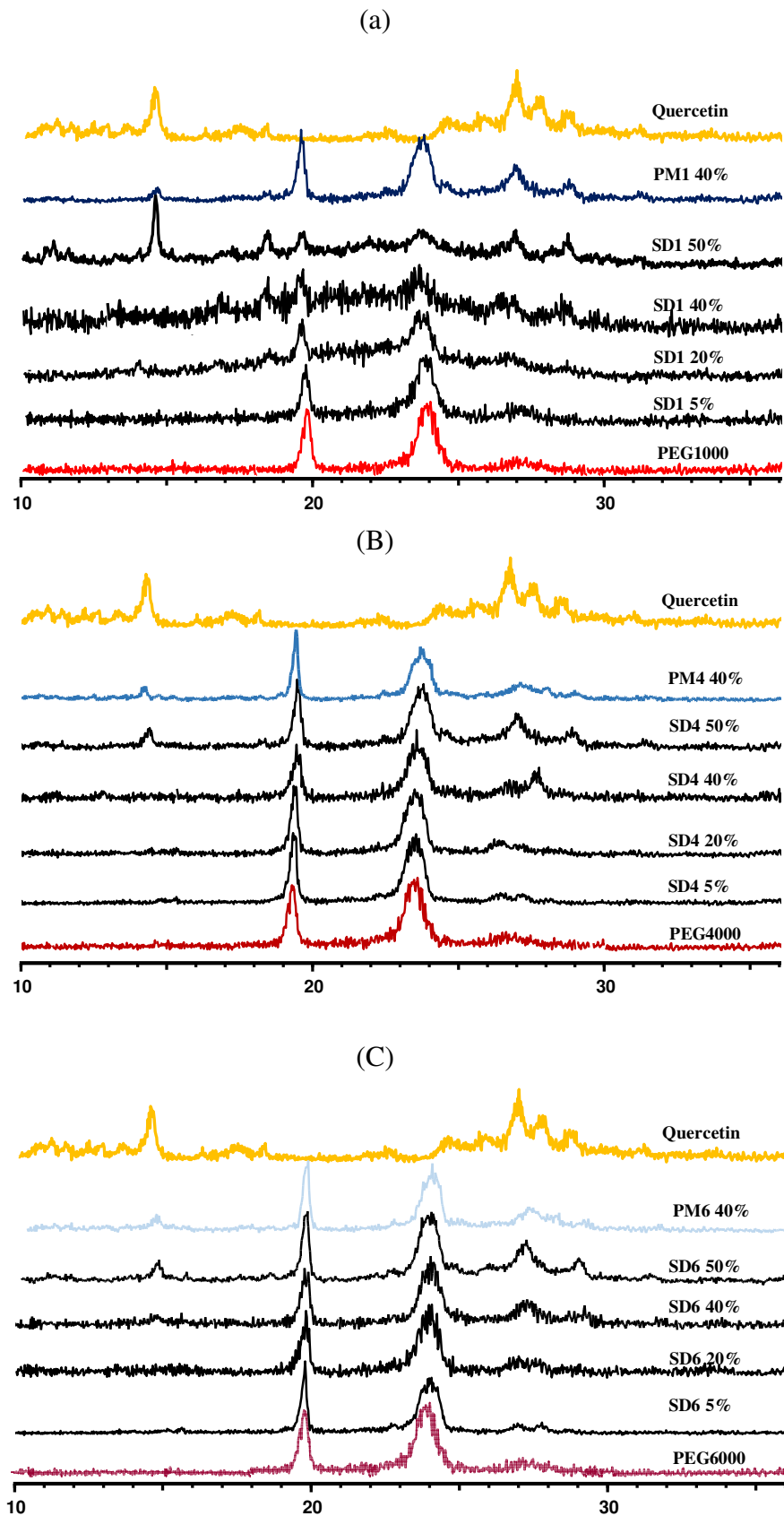
Product	Group contribution methods						Density (kg/m ³)	V _m (cm ³ /mol)
	Small		Hoy		Van Krevelen			
	δ (MPa ^{0.5})	χ	δ (MPa ^{0.5})	χ	δ (MPa ^{0.5})	χ		
PEG 1000	19.1	4.6	21.5	2.2	23.4	0.9	1222	869
PEG 4000	18.9	4.9	21.1	2.6	22.5	1.5	1224	3268
PEG 6000	18.8	5.0	21.2	2.5	22.4	1.6	1223	4906

639

640

642 **Fig. 1**

643 Entropy (a) and free energy of mixing Quercetin with PEG1000 (dotted lines), PEG4000 (long hashed
 644 lines), and PEG6000 (solid lines), as a function of volume fraction polymer, using solubility parameters
 645 from the method of Small (b), Hoy (C) and van Krevelen (d).

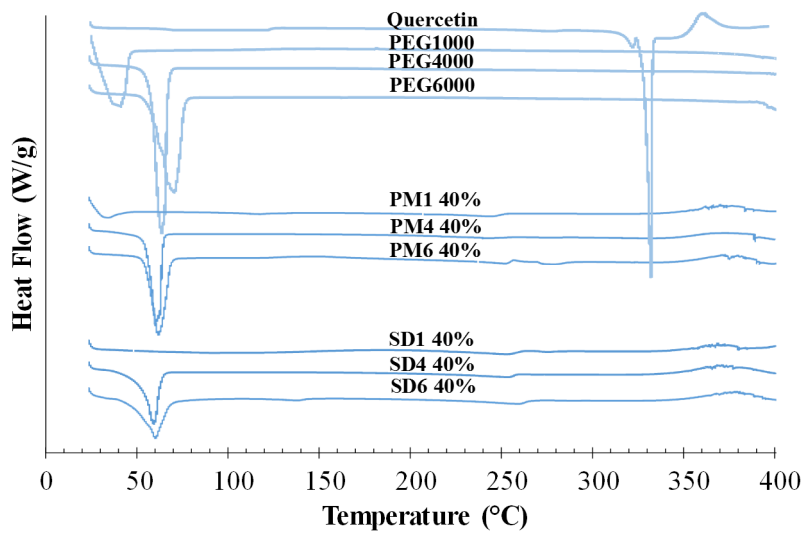
647 **Fig. 2**

648 X-ray diffraction analysis of quercetin, PEGs, Physical Mixtures (PM) and solid dispersions (SD) of
 649 varying composition; PM1, PM4 and PM6 correspond to quercetin physical mixtures with PEG1000,
 650 PEG4000 and PEG6000 respectively; SD1, SD4 and SD6 correspond to quercetin solid dispersions with
 651 PEG1000, PEG4000 and PEG6000 respectively

652

653

654

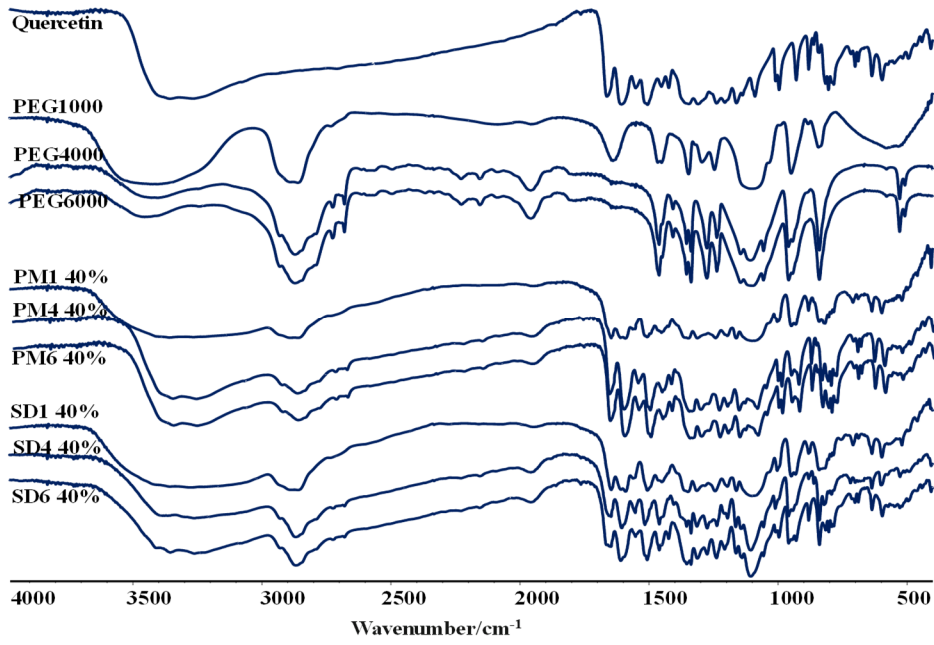


655

656 **Fig. 3**

657 DSC of quercetin, physical mixtures quercetin-PEG1000 (PM1), quercetin-PEG4000 (PM4) and
658 quercetin-PEG6000 (PM6); and solid dispersions quercetin-PEG1000 (SD1), quercetin-PEG4000 (SD4)
659 and quercetin-PEG6000 (SD6) at composition of 40%

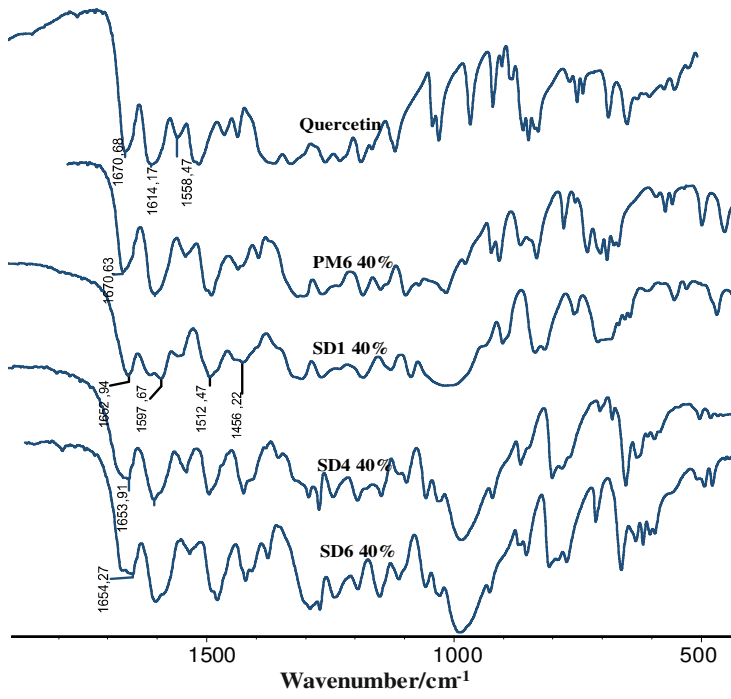
660



662

663 **Fig. 4**

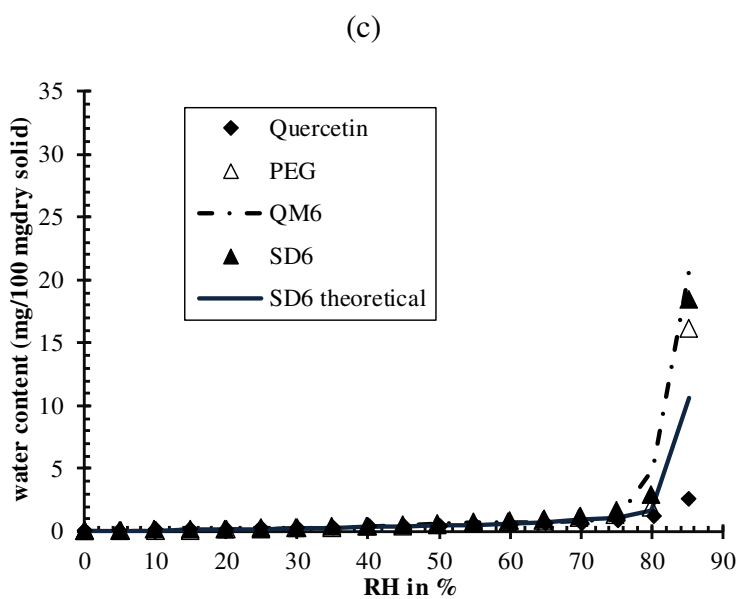
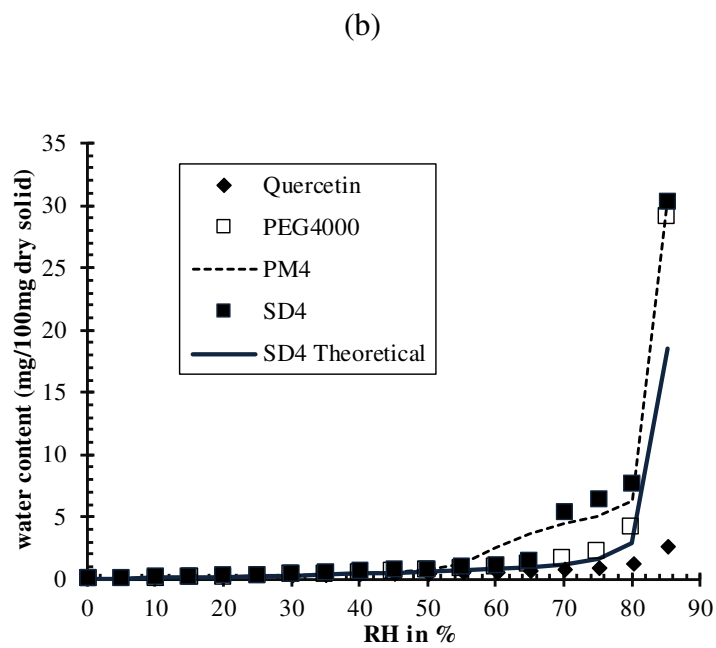
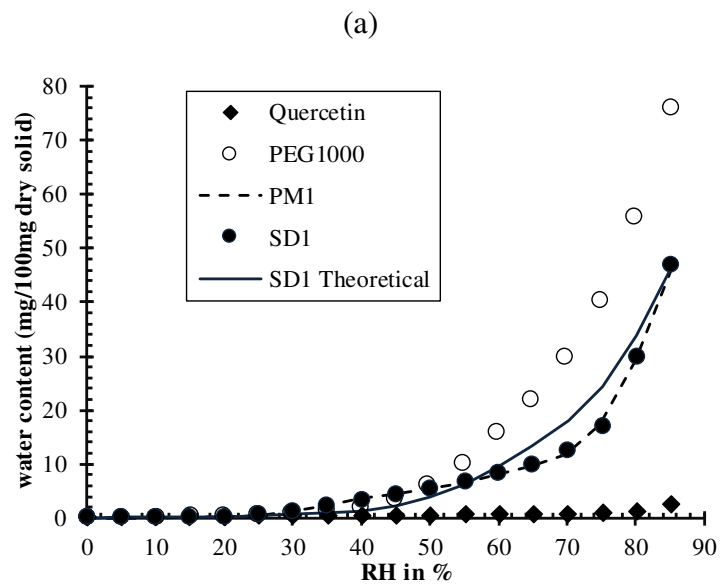
664 FTIR spectra of quercetin, physical mixtures quercetin-PEG1000 (PM1), quercetin-PEG4000 (PM4) and
665 quercetin-PEG6000 (PM6); and solid dispersions quercetin-PEG1000 (SD1), quercetin-PEG4000 (SD4)
666 and quercetin-PEG6000 (SD6) at composition of 40%



668

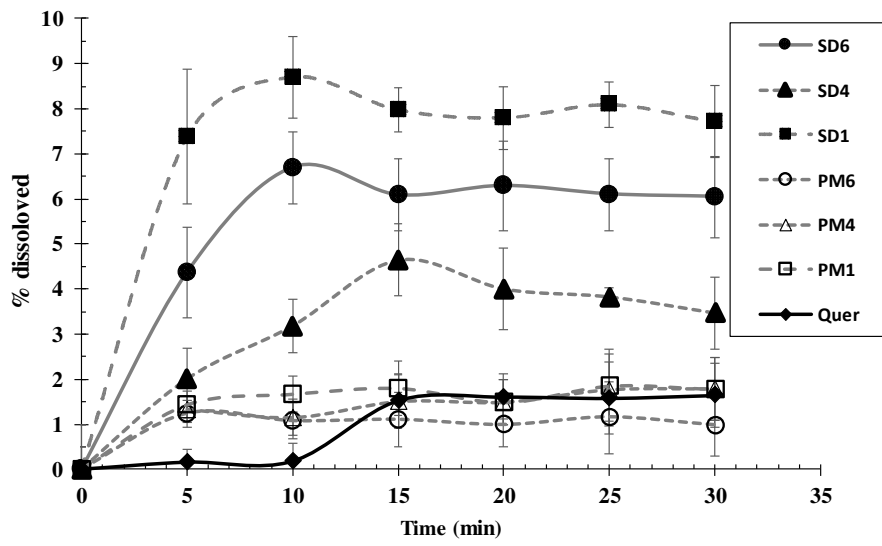
669 **Fig. 5**

670 FTIR spectra, for wavenumber between 450 and 1900 cm⁻¹, of quercetin, physical mixture quercetin-
 671 PEG6000 (PM6); and solid dispersions quercetin-PEG1000 (SD1), quercetin-PEG4000 (SD4) and
 672 quercetin-PEG6000 (SD6), at composition of 40%



673 **Fig. 6**

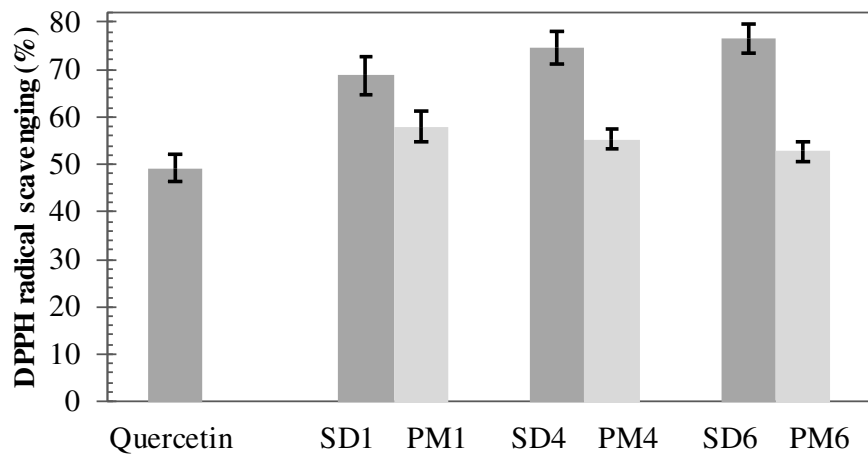
674 Vapor sorption isotherms at 25 °C of SDs (40%), quercetin and various MW PEGs measured by
 675 automated gravimetric moisture analysis SPS. (a) quercetin-PEG1000 (SD1), (b) quercetin-PEG4000
 676 (SD4), (c) quercetin-PEG6000 (SD6). Solid lines and dashed lines are isotherms of quercetin-PEG
 677 theoretical and of physical mixtures PMs respectively.



678

679 **Fig. 7**

680 Dissolution profile of quercetin in physical mixture with PEG1000 (PM1), PEG4000 (PM4) and
 681 PEG6000 (PM6); and in solid dispersion with PEG1000 (SD1), PEG4000 (SD4) and PEG6000 (SD6), at
 682 composition of 40%.



683

684 **Fig. 8**

685 In vitro antioxidant activity of quercetin, physical mixtures of quercetine with PEG1000 (PM1),
686 PEG4000 (PM4) and PEG6000 (PM6) and solid dispersions of quercetine-PEG1000 (SD1), quercetin-
687 PEG4000 (SD4) and quercetine-PEG6000 (SD6), at 40 % (w/w).

688

689

690